Graphene quantum Hall effect devices for AC and DC resistance metrology

Mattias Kruskopf*, Dinesh K. Patel§,†, Chieh-I Liu§,‡, Albert F. Rigosi§, Randolph E. Elmquist§, Yicheng Wang§, Stephan Bauer*, Yefei Yin*, Klaus Pierz*, Eckard Pesel*, Martin Götz* and Jürgen Schurr*

*Physikalisch-Technische Bundesanstalt (PTB), Bundesallee 100, Braunschweig, 38116, Germany

§National Institute of Standards and Technology (NIST), 100 Bureau Drive, Stop 8171, Gaithersburg, MD, 20899, USA

†Graduate Institute of Applied Physics, National Taiwan University, Taipei 10617, Taiwan

‡University of Maryland, Department of Chemistry and Biochemistry, College Park, MD, 20742, USA

***Abstract* — The frequency dependence of the quantized Hall resistance at alternating current results from capacitive losses inside the sample as well as between the sample and external parts. In this joint effort, we report on ac quantum Hall measurements of a graphene-based Hall bar using superconducting contacts and a novel contact design approach.**

***Index Terms* — electrical measurement standards, ac quantized Hall resistance, epitaxial graphene.**

I. Introduction

The fundamental nature of the quantum Hall effect allows for the realization of an electrical standard for the direct current (dc) resistance as well as for the impedance, capacitance, and inductance [1]–[3]. To accelerate the worldwide adoption of these techniques, National metrology institutes are investigating the deviation of the quantized Hall resistance (QHR) at alternating current (ac) from the value measured at dc. Parasitic capacitances were identified to be the reason for the observed offsets, which can be compensated using externally applied shields [4].

In this paper, we report on a joint effort of the PTB and the NIST to characterize an epitaxial graphene-based Hall bar using superconducting contacts and an optimized contact geometry to identify measurement conditions and sample characteristics that are critical to the measurement precision [5].

II. DC Measurements

Figure 1(a) shows the sample design, the measurement configuration and dominating parallel capacitances under ac conditions. The magnetotransport properties at direct current were pre-characterized using a current source and a nano voltmeter for magnetic flux densities between $B = 0$ T to $B = 12$ T. Figure 1(b) shows that due to the low carrier density of $n = 6.6\times10^{10}$ cm^{-2}, the resistance plateau started at around $B = 1$ T and the longitudinal resistance, measured with current reversal to reject thermal voltages, was within the setups the noise floor for $B > 2$ T. The sample was then characterized with a cryogenic current comparator at $B = 7$ T. The longitudinal resistance was found to be (465 ± 1.5) μΩ on the low potential side and (694 ± 1.5) μΩ on the high potential side (type A uncertainty $k = 1$).

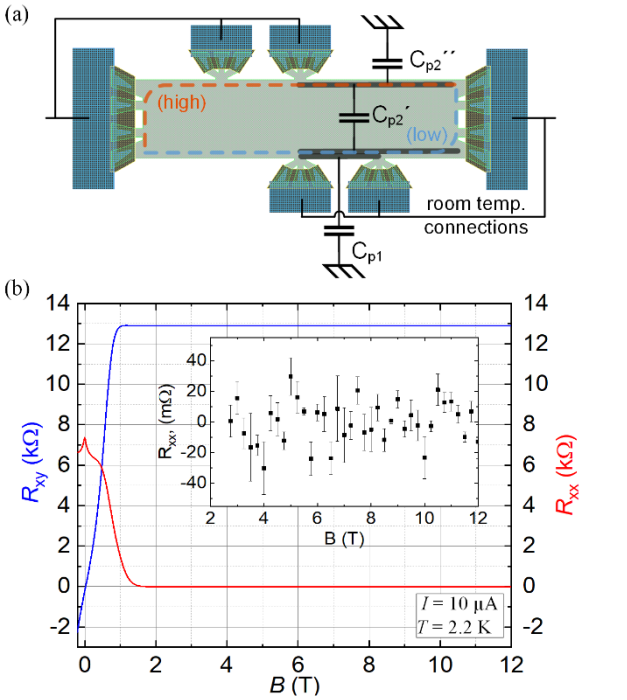

Fig. 1. (a) The drawing shows the sample design as well as indicates the origin of parallel capacitances of the Hall and longitudinal resistance measurements at ac. (b) Characterization of dc magneto transport properties. The carrier density n and mobility μ are 6.6×10^{10} cm^{-2} and 12883 cm²/Vs, respectively. The inset indicates a vanishing of the longitudinal resistance at magnetic flux densities around $B = 2$ T. The error bars represent the standard deviation determined from three measurements.

III. AC Measurements

The deviation of the Hall resistance at ac from the dc value R_H shows a linear frequency dependence with a slope of (81.7 ± 1.5) × 10^{-9} / kHz (see Fig.2, top). The parallel capacitance C_{p2} (bottom) is measured at the pair of Hall contacts and is

978-1-7281-5898-3/20/$31.00 ©2020 IEEE

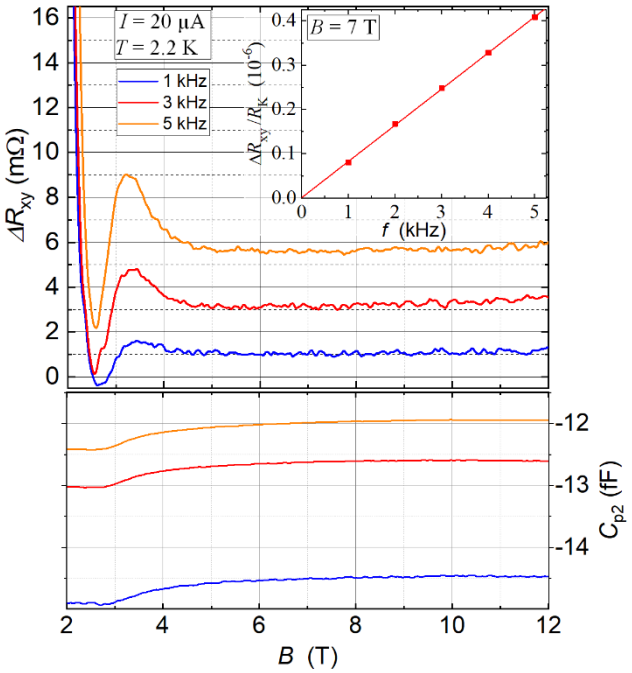

Fig. 2. The deviation of the Hall resistance ΔR_{xy} at ac from the dc value R_H (top) with a slope of 81.7 ± 1.5 × 10^{-9} /kHz (see inset) and corresponding magetocapacitance measurements (bottom).

composed of the two components C_{p2}' and C_{p2}'' where C_{p2} = C_{p2}'- C_{p2}''. While the absolute value of C_{p2} has a large uncertainty of 58 fF, the shape of the magnetic field dependence can still be precisely measured. The graph shows that C_{p2} increases in the beginning of the resistance plateau and becomes mostly flat for $B \geq 6$T, reflecting the changes in the areas of compressible and incompressible states inside the QHR sample and a dominating contribution from C_{p2}'' compared to C_{p2}'. Figure 3 shows the frequency dependence of the longitudinal resistance (top) and the parallel capacitance C_{p1} (bottom) measured at the same contact pair. The upwards bending of the longitudinal resistance curves at higher magnetic flux densities and the absence of a clear flat region indicates a non-zero longitudinal resistance at $f = 0$ Hz in agreement with the results of the cryogenic current comparator. Interestingly, the increase of the longitudinal resistance at higher magnetic fields seems to be associated with an increase of C_{p1}.

IV. Conclusion and Outlook

The applied sample design resulted in a Hall resistance with a positive frequency dependence. Previously published ac QHR measurements using graphene Hall bars [6] showed a positive frequency dependence in the case of much larger sample dimensions (e.g. 2600 µm × 800 µm) and higher current. By further investigating the frequency dependence with respect to the charge carrier density and the applied current as well as by applying the double-shield technique, we are aiming to find favorable conditions for precise ac QHR measurements.

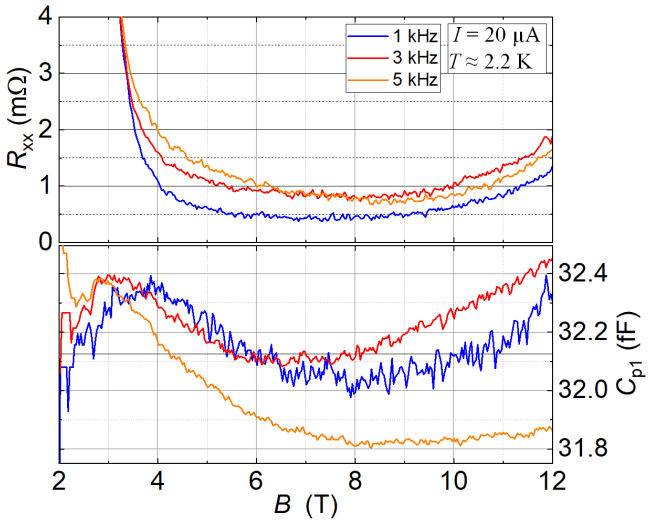

Fig. 3. Longitudinal resistance (top) and magnetocapacitance measurements (bottom) at ac and different frequencies at the low potential side.

Acknowledgment and Funding

This work was supported by the Joint Research Project GIQS (18SIB07). This project received funding from the European Metrology Program for Innovation and Research (EMPIR) co-financed by the Participating States and from the European Unions' Horizon 2020 research and innovation program. The work of D. K. Patel at NIST was made possible by arrangement with Prof. C.-T. Liang of the National Taiwan University.

References

[1] J. Schurr, V. Bürkel, and B. P. Kibble, "Realizing the farad from two ac quantum Hall resistances," *Metrologia*, vol. 46, no. 6, pp. 619–628, Dec. 2009.

[2] J. Schurr, F. Ahlers, and B. P. Kibble, "The ac quantum Hall resistance as an electrical impedance standard and its role in the SI," *Meas. Sci. Technol.*, vol. 23, no. 12, p. 124009, Dec. 2012.

[3] A. Hartland, "The Quantum Hall Effect and Resistance Standards," *Metrologia*, vol. 29, no. 2, pp. 175–190, Jan. 1992.

[4] J. Schurr, B. P. Kibble, G. Hein, and K. Pierz, "Controlling losses with gates and shields to perfect a quantum Hall impedance standard," *IEEE Trans. Instrum. Meas.*, vol. 58, no. 4, pp. 973–979, 2009.

[5] M. Kruskopf *et al.*, "Two-Terminal and Multi-Terminal Designs for Next-Generation Quantized Hall Resistance Standards: Contact Material and Geometry," *IEEE Trans. Electron Devices*, pp. 1–5, 2019.

[6] C.-C. Kalmbach, *AC-Quanten-Hall-Effekt und 1/f -Rauschen in epitaktischem Graphen*, E 113. PTB Bericht, 2017.